Materials Physics and Mechanics 44 (2020) 332-347 Received: September 19, 2018

STRUCTURAL BEHAVIOR OF FG-CNT CYLINDRICAL PANEL: INFLUENCE OF NON-UNIFORM TEMPERATURE FIELD

Vinod Bhagat[1], P. Jeyaraj[2*]

[1]Institute of Shipbuilding Technology, Vasco-da-Gama, Goa, India, 403802

[2]Department of Mechanical Engineering, National Institute of Technology, Karnataka, India

*e-mail: pjeyaemkm@gmail.com

Abstract. In this study, the influence of non-uniform temperature field and temperature-dependent properties on buckling and free vibration behavior of functionally graded carbon nanotube (FG-CNT) reinforced composite cylindrical panel is investigated. For the structural analysis, the finite element method and modal assurance criterion (MAC) analysis are performed. It is found that the temperature-dependent properties and nature of temperature variation fields affect the thermal buckling strength of the panel greatly. The results from MAC analysis reveals that the influence of temperature and nature of temperature variation on buckling and free vibration modes are significant. Further, it is also found that variations in frequencies and associated modes are significant at a temperature closer to buckling temperature.

Keywords: carbon nanotube, non-uniform heating, cylindrical panel, finite element method, thermal buckling, free vibration

1. Introduction

The significant amount of research is being carried out on FG-CNT polymer nano-composite structures in order to characterize their mechanical characteristics under various loading conditions. The reason behind this is the advantages of high strength, stiffness, and less weight associated with the newly developed advanced material FG-CNT. The functionally graded cylindrical panel has found its application in the components of highly inflammable fluid storage tanks, supersonic and hypersonic aircrafts, nuclear reactors, and jet engine exhausts. Thin cylindrical panel-like structures utilized in aircrafts with high-speed, rockets, reactor vessels, spacecraft's, and turbines during their service are subjected to an extreme thermal load. Stresses set up due to thermal load results in thermal buckling and also influences the dynamic characteristics of the structures. Hence, buckling and dynamic characteristics of a functionally graded cylindrical panel under thermal load turn out to be a crucial element in their design process. [1] investigated buckling behavior of functionally graded cylindrical shells under thermal and mechanical load using first-order shear deformation theory and element-free kp-Ritz method.

Vibration characteristics of functionally graded material plates under thermomechanical load were analyzed by [2] using a finite-element method based on higher-order shear deformation theory. Composite cylindrical shells reinforced by carbon nanotubes were analyzed by [3] under uniform temperature rise. The governing equations based on higher-order shear deformation theory was used to study the buckling and post-buckling behavior. He found that buckling and post-buckling strength of the shell under thermal load can be increased by functionally graded reinforcement. Refined plate theories with four

http://dx.doi.org/10.18720/MPM.4432020_6

various variables were employed by [4] to investigate the free vibration behavior of functionally graded plates with temperature-dependent properties. Functionally graded cylindrical panels were analyzed by [5] for its thermal buckling strength using the differential quadrature method. Panel subjected to uniform and variable temperature rise in the radial and axial direction was considered. [6] employed a simple shear deformation theory to investigate the thermal stability of functionally graded sandwich plates.

[7] analyzed FG-CNT composite cylindrical panels for its flexural strength and free vibration by employing first order shear deformation theory. Eshelby-Mori-Tanaka approach was used to calculate the material properties of nanocomposite panels. A mesh-free kp-Ritz method was used by [8] to study the influence of static and periodic axial force on the dynamic stability of carbon nanotube-reinforced functionally graded cylindrical panels. [9] investigated the free vibration characteristics of single-walled carbon nanotubes reinforced composite plates. The refined rule of the mixture approach that involves the efficiency parameters was used to calculate the properties of the composite material. Further, they found that the frequencies of the panel can be enhanced by increasing the volume fraction of carbon nanotubes. [10] investigated the buckling and post buckling behavior of composite laminates with constant and variable stiffness having straight and curvilinear fibers respectively. [11] employed molecular dynamics simulations to investigate the elastic properties of the CNT reinforced epoxy/CNT composite.

Very few literatures (e.g. [12-17]) highlighted on the free vibration behavior of cylindrical shells and plates under thermal load. [12] investigated the influence of the thermal environment on the vibration behavior of nanocomposite cylindrical shells. [13] used finite element method to investigate the free vibration and buckling behavior of plate under non-uniform thermal load. The finite element approach was used by [14] to investigate the buckling and free vibration behavior of FGCNT reinforced polymer composite plate exposed to non-uniform temperature fields. [15-16] carried out experiments on metal and composite beams and showed that structural behavior of heated structure is very sensitive to the nature of temperature variation. [17-19] investigated non-uniformly heated isotropic and laminated composite cylindrical panels respectively. They used finite element approach to investigate the influence of thermal load on buckling and the free vibration behavior of cylindrical panels under thermal load.

The review of the literature indicates that FG-CNTRC cylindrical panel exposed to non-uniform temperature field with temperature-dependent properties have not been analyzed for its detailed study on combined buckling and free vibration behavior. However, some literature on FG-CNTRC cylindrical shells under the thermal environment is confined to either uniform or variation in the thickness direction and also with temperature-independent properties. Whereas in some of the literature temperature-dependent properties are considered but only at particular values of temperature (300K, 400K, 500K). In reality, due to un-symmetric geometric variation and the nature of heat source, the panels are exposed to arbitrarily changing non-uniform temperature variation fields and different temperatures. For example, panels employed in aerospace vehicles, electronic circuit board, columns of the heating furnace, car panels situated close to the engine, components of rockets, missiles, and nuclear vessels. Due to the non-uniform nature of the temperature distribution field, thin cylindrical shell structures are highly susceptible to thermal buckling. Further, stresses resulted due to non-uniform thermal load, and temperature-dependent properties influence the free vibration behavior of the structures significantly. Thus, the influence of non-uniform temperature variation fields and temperature-dependent properties on combined buckling and vibration behavior of cylindrical panel is vital in the design stage and the present study focuses on these aspects.

2. Modeling of material for FG-CNT Reinforced Composite

CNTRC cylindrical panel analyzed in the present study is assumed to be made from a blend of single-walled carbon nano-tubes (SWCNTs) and isotropic matrix. The SWCNT reinforcement is either functionally graded (FG) or uniformly distributed (UD) through the thickness direction. The present study focuses on four types of through-thickness functionally graded distribution patterns of carbon nanotubes namely UD, FG-X, FG-O, and FG-V as shown in Fig. 1.

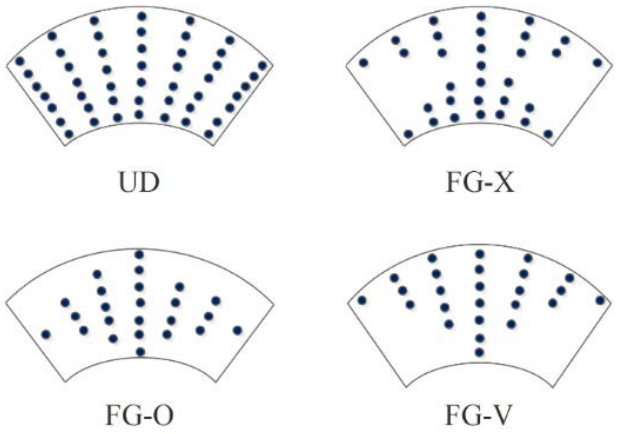

Fig. 1. Configurations of CNTRCs

The main issue with CNTRCs is to get effective material properties. Numerous micromechanical models have been evolved to anticipate the properties of CNT-reinforced nanocomposites, such as the Mori–Tanaka scheme [20,21] and the rule of mixture [22,23]. The Mori-Tanaka scheme is employed for nanoparticles but the rule of mixture is identified as a simple model and also convenient to use while predicting the overall material properties. The accuracy of the rule of mixture was presented and a significant synergism between the Mori-Tanaka scheme and the rule of mixture for functionally graded ceramic-metal beams were reported in [24]. Further, a comparative study was conducted between Eshelby–Mori–Tanaka scheme and the extended rule of mixture for the vibration analysis of continuously graded carbon nanotubes reinforced cylindrical panels in [25]. In the present analysis the rule of mixture is used to calculate effective properties.

Rule of Mixture: According to the extended rule of mixture, effective material properties of CNTRC plates can be expressed as [26]

$$E_{11} = \eta_1 V_{CNT} E_{11}^{CNT} + V_m E^M,$$
$$\frac{\eta_2}{E_{22}} = \frac{V_{CNT}}{E_{22}^{CNT}} + \frac{V_m}{E^M}, \quad (1)$$
$$\frac{\eta_3}{G_{12}} = \frac{V_{CNT}}{G_{12}^{CNT}} + \frac{V_m}{G^M}.$$

In Eq. 1, η_1, η_2 and η_3 are the efficiency parameters introduced to consider load transfer between the nanotubes and polymeric phases (e.g. the surface effect, strain gradient effect, and intermolecular coupling effect) and other effects on the effective material properties of CNTRCs. [26] computed the CNT efficiency parameter by matching Young's moduli E_{11} and E_{22} of CNTRCs obtained by the rule of mixture to MD results of [27]. Besides, in Eq. 1, Young's modulus and shear modulus of SWCNTs are denoted by E_{11}^{CNT}; E_{22}^{CNT} and G_{12}^{CNT}, respectively. Furthermore, the properties of the isotropic matrix are given by E^M and G^M. V_{CNT} and V_m represents the volume fraction of CNTs and matrix, respectively and follows the relation

$$V_{CNT} + V_m = 1. \quad (2)$$

In the present study, FG-CNTRC panel with three different types of CNTs distributions [28] through the thickness directions has been analyzed. The volume fraction of CNTs in each lamina as a function of thickness coordinate for the three different types of CNTs distributions [28] are as follows

$$V_{CNT}(Z) = \begin{cases} V_{CNT}^{*} & (UD) \\ 2\left(1 - \frac{|2z|}{h}\right) V_{CNT}^{*} & (FG-O) \\ 2\left(\frac{2|z|}{h}\right) V_{CNT}^{*} & (FG-X) \\ \left(1 + \frac{2z}{h}\right) V_{CNT}^{*} & (FG-V) \end{cases} \quad (3)$$

$$V_{CNT}^{*} = \frac{W_{CNT}}{W_{CNT} + (\rho^{CNT}/\rho^{m}) - (\rho^{CNT}/\rho^{m}) W_{CNT}}, \quad (4)$$

where mass fraction and mass density of the CNTs are given by W_{CNT} and ρ^{CNT} respectively, whereas the mass density of the isotropic matrix is given by ρ^{m}. The thermal expansion coefficients in longitudinal (α_{11}), and transverse directions (α_{22}), Poisson's ratio (ν_{12}) and the overall mass density ρ are given by following Equations.

$$\nu_{12} = V_{CNT}\nu_{12}^{CNT} + V_{m}\nu^{m}, \quad (5)$$

$$\rho = V_{CNT}\rho^{CNT} + V_{m}\rho^{m}, \quad (6)$$

$$\alpha_{11} = V_{CNT}\alpha_{11}^{CNT} + V_{m}\alpha^{m}, \quad (7)$$

$$\alpha_{22} = (1 + \nu_{12}^{CNT}) V_{CNT}\alpha_{22}^{CNT} + V_{m}\alpha^{m} - \nu_{12}\alpha_{11}. \quad (8)$$

3. Finite element formulation

The present study uses finite element method to evaluate critical buckling temperature, fundamental buckling mode shape, natural frequencies, and corresponding free vibration mode shapes of FG-CNTRC cylindrical panel under non-uniform heating conditions. The cylindrical panel considered for the analysis is shown in Fig. 2 with a length (*L*), width (*S*), thickness (*h*) and mean radius of curvature (*R*). Structures under the thermal environment with a restrained boundary for free expansion experience thermal stress. Membrane forces developed due to thermal stress influence the lateral deflection of the structure and this is analyzed by using structural analysis.

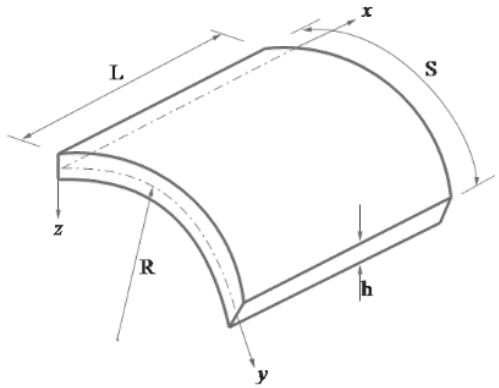

Fig. 2. Geometry of the Cylindrical panel

Structural analysis. By employing the static analysis, stress developed in the structure under thermal load is computed. By following the usual finite element procedure, structural stiffness matrix, $[K]$, geometric stiffness matrix, $[K_{\sigma}]$ is obtained [29]. The governing equation of the whole panel for static analysis is given by

$$[K]\{U\} = \{F\}, \quad (9)$$

where $[K]$ is the structural stiffness matrix, $\{F\}$ is the thermal load vector and $\{U\}$ is the nodal displacement vector.

Evaluating the buckling temperature of the panel with temperature-independent properties. Buckling analysis for a panel with temperature-independent properties is performed by solving the following governing equation

$$([K] + \lambda_i[K_\sigma])\{\psi_i\} = 0\ , \tag{10}$$

where λ_i is the eigenvalue and $\{\psi_i\}$ is the corresponding eigenvector for i^{th} buckling mode. The product of the temperature rise, ΔT (above ambient temperature) and the lowest eigenvalue, λ_i gives the critical buckling temperature, T_{cr} (i.e., $T_{cr} = \lambda_1 \Delta T$).

Evaluating buckling temperature of panel with temperature dependent properties. Buckling analysis for a panel with temperature dependent properties is performed by using following iterative process [30].

1. Initially obtain the buckling temperature (ΔT_{cr}) for the panel with temperature-independent material properties at reference temperature T_0 using Eq.10.
2. Update stiffness matrix [K] by changing the property values at $T = T_0 + \Delta T_{cr}$ to evaluate a new buckling temperature.
3. Repeat Step 2 till the thermal buckling temperature converges to a prescribed error tolerance as given below

$$\varepsilon = \left|\frac{\Delta T_{cr}^{(i+1)} - \Delta T_{cr}^{(i)}}{\Delta T_{cr}^{(i)}}\right| \leq 10^{-4}\ . \tag{11}$$

Free vibration frequencies under thermal load. In order to find the effect of thermal stress on the natural frequencies and its associated mode shapes at a particular elevated temperature, pre-stressed modal analysis is carried out by using Eq. 12.

$$\left(([K] + [K_\sigma]) - \omega_k^2[M]\right)\{\phi_k\} = 0, \tag{12}$$

where, ω_k is the natural frequency of the pre-stressed structure, $\{\Phi_k\}$ the corresponding mode shape, and [M] is the structural mass matrix.

Modal assurance criteria (MAC) analysis. To analyze the influence of different temperature fields on the buckling and vibration mode shape of the panel, a modal assurance criterion is employed. Modal assurance criteria ([31] Pastor et al. (2012)) is carried out using the following equation.

$$MAC(\{\varphi\}_r, \{\varphi\}_s) = \frac{|\{\varphi\}_r^{*t}\{\varphi\}_s|^2}{(\{\varphi\}_r^{*t}\{\varphi\}_r)(\{\varphi\}_s^{*t}\{\varphi\}_s)}\ , \tag{13}$$

where $\{\varphi\}_r$= modal vector for mode 'r', $\{\varphi\}_s$= modal vector for mode 's'.

Temperature Fields. In the present study, three types of 1-D temperature fields varying along the length and a 2-D inplane temperature field are considered to analyze the nature of temperature variation. The panel under uniform temperature rise above ambient temperature is also investigated, so that influence of change in temperature distribution field from uniform to non-uniform can be studied. Temperature distribution field along with their mathematical expression is given below,

1. Case (a): Uniform temperature field, $(T(x) = T_{max})$;
2. Case (b): Decreasing temperature field, modeled by heating at one edge of the panel, $(T(x) = T_{max}[1 - (\frac{x}{L})])$;
3. Case (c): Decrease and increase temperature fields simulated by heating at two opposite edges of the panel $(T(x) = T_{max}[1 - (1 - abs(1 - \frac{2x}{L}))])$;
4. Case (d): Increase and decrease temperature fields modeled by heating at the middle of the panel $(T(x) = T_{max}[1 - abs(1 - \frac{2x}{L})])$;
5. Case (e): Camel hump temperature field, $(T(x, y) = T_{max}[sin(\pi y/S) \times sin(\pi x/L)])$.

The present study deals with a thin cylindrical panel, thus it is assumed that change in temperature through thickness direction is negligible. Temperature distribution field profiles of the panel for Cases (a)-(e) are shown in Table 1.

Table 1. Different temperature distribution field analyzed

Case(a)	Case(b)	Case(c)	Case(d)	Case(e)
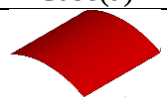	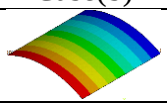	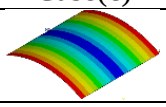	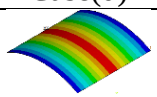	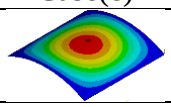

*Blue: ambient temperature; Red: 1^{o}C above ambient temperature and others in-between

4. Validation study

Critical buckling temperature. Cylindrical shell made of functionally graded materials, investigated by [32] for the thermal buckling strength with temperature-dependent (TD) properties is considered for the validation. [32] analyzed Si_3N_4/ SUS304 with proportionate dimensions of the panel are L = $\sqrt{300}$Rh, R/h = 400. [32] used an analytical method, while the present method uses commercial finite element software, ANSYS. An eight noded layered structural shell element formulated based on first order shear deformation theory, SHELL 281 is used. Critical buckling temperature evaluated using the present method shows good agreement with the results reported by [32] as seen in Table 2.

Table 2. Comparison of buckling strength of the FGM panel

Volume fraction index	Critical buckling temperature(K)		% diff.
	[32]	Present	
0	392.79	393.95	0.29
0.2	402.31	401.86	0.11
0.5	412.55	411.09	0.35
1	424.15	421.61	0.60

Evaluation of Free Vibration Frequencies. CNTs reinforced cylindrical panel analyzed by [7] for its free vibration frequencies is considered for the validation. The dimension of the panel investigated by [7] are h=0.002 m, h/R=0.002, L/R=0.1 and θ =0.1 rad. For comparison, two types of CNTs distribution, namely UD and FG-X are considered with 0.12 of CNTs volume fraction. The present method uses ANSYS, whereas [7] used an approach based on first order shear deformation theory. Extracted non-dimensional natural frequencies for a simply supported cylindrical shell, using present study matches very well with that of results reported by [7] as shown in Table 3. Non-dimensional natural frequency is given by

$$\widehat{\omega} = \omega(\frac{S^2}{h})\sqrt{\frac{\rho^M}{E^M}}\,.$$

Table 3 Comparison of Non-dimensional natural frequencies with [7]

Modes	UD			FG-X		
	[7]	Present	% diff.	[7]	Present	% diff.
1	17.85	17.79	0.33	21.24	21.56	1.51
2	22.07	22.76	3.12	25.10	26.08	3.90
3	33.29	34.79	7.74	35.94	37.76	5.06
4	51.77	53.98	4.26	54.54	57.11	4.71
5	65.12	63.80	2.02	76.76	75.95	1.06

5. Results and discussion

The effect of thermal stress developed due to non-uniform heating on buckling and free vibration characteristics of FG-CNT reinforced cylindrical panel is investigated. The influence of important geometrical parameters, different boundary constraints, and temperature distribution fields are analyzed. Throughout the analysis, a cylindrical panel with the thickness (h) = 0.001m, thickness ratio (S/h) = 100, and curvature ratio (R/S) =2 has been considered otherwise it is mentioned. For the present simulation, polymethyl methacrylate, referred to as PMMA, is chosen as the matrix material with properties $E_m = (3.52 - 0.0034T)$ GPa, ν_m = 0.34 and α_m = $45(1 + 0.0005\Delta T)10^{-6}$/K. In the calculation of elasticity modulus of the matrix, the elevated temperature $T = T_0 + \Delta T$ where T_0 = 300 K is the reference temperature. For reinforcement, (10, 10) armchair single-walled carbon nanotubes (SWCNT) is selected. Poisson's ratio, shear modulus, elasticity modulus and thermal expansion coefficient of SWCNT are assumed to be temperature-dependent. To carry out a temperature-dependent investigation, the thermo-mechanical properties of (10, 10) armchair SWCNT are predicted as a function of temperature using a third order interpolation [33]. Change in thermo-mechanical properties of (10, 10) armchair SWCNT with temperature for a range of 300 ≤ T≤ 700 is given in Eq. 14.

$$
\begin{aligned}
&E_{11}^{CNT}(T)[Tpa] = 6.3998 - 4.338417 \times 10^{-3}T + 7.43 \times 10^{-6}T^2 - 4.458333 \times 10^{-9}T^3,\\
&E_{22}^{CNT}(T)[Tpa] = 8.02155 - 5.420375 \times 10^{-3}T + 9.275 \times 10^{-6}T^2 - 5.5625 \times 10^{-9}T^3,\\
&G_{12}^{CNT}(T)[Tpa] = 1.40755 + 3.476208 \times 10^{-3}T - 6.965 \times 10^{-6}T^2 + 4.479167 \times 10^{-9}T^3,\\
&\alpha_{11}^{CNT}(T) = (-1.12515 + 0.02291688T - 2.887 \times 10^{-5}T^2 + 1.13625 \times 10^{-8}T^3) \times \alpha_0,\\
&\alpha_{22}^{CNT}(T) = (5.43715 + 9.84625 \times 10^{-4}T - 2.9 \times 10^{-7}T^2 + 1.25 \times 10^{-11}T^3) \times \alpha_0,\\
&\alpha_0 = 10^{-6}/K,\\
&\nu_{12}^{CNT} = 0.175.
\end{aligned}
\tag{14}
$$

The present analysis mainly focuses on four different functionally graded configurations of CNTs distribution such as UD, FG-X, FG-O, and FG-V with three different volume fractions (0.12, 0.17, 0.28) to investigate the influence of functional grading and volume fraction of CNTs on the buckling and free vibration characteristics of non-uniformly heated CNTRC cylindrical panel. In Figure 2, UD represents the uniform distribution of CNTs, FG-X represents volume fraction of CNTs increasing symmetrically from the mid-plane and FG-O represents volume fraction of CNTs decreasing symmetrically from the mid-plane. To know the effect of un-symmetry associated with CNTs distribution, FG-V is considered. The CNTs efficiency parameters, η_i for different volume fractions are η_1 = 0.137 and η_2 =1.022 for V_{CNT}^* = 0.12, η_1 = 0.142 and η_2 =1.626 for V_{CNT}^* = 0.17 and η_1 = 0.141 and η_2= 1.585 for V_{CNT}^* = 0.28 and η_2=η_3. In order to investigate the influence of boundary constraints, panels under CCCC and CCFC (C-clamped edge and F-free edge) are considered. The first letter in these boundary constraints is associated with the forefront curved edge at x= 0 in order.

Non-dimensional critical buckling temperature used in the present analysis is given below $T_{cr}^* = T_{cr} \times \alpha_0 \times 10^{-3}$.

Buckling Behavior. The influence of thickness ratio and in-plane temperature fields on the buckling strength is carried out on a panel with different thickness ratios. Figure 3 shows the effect of the thickness ratio on the buckling strength of the CNTRC panel. From Figure 3, it is observed that the buckling strength of the panel decreases with the increase in thickness ratio irrespective of temperature fields. This behavior of the panel is mainly due to the reduction in both structural stiffness and membrane force with the increase in thickness ratio. The panel exposed to Case(a) temperature field, has the lowest buckling strength whereas panel under Case(e) temperature field has highest buckling strength. This is due to the fact that the panel under Case(a) temperature field produces more membrane forces as the total area is exposed to peak temperature. It is also observed that the buckling strength of the panel with temperature-dependent (TD) properties is lower compared to the panel with temperature-

independent (TID) properties. Material properties of the panel deteriorate with the increase in temperature, thus buckling strength of the panel decreases. Variation in the buckling strength of the panel with TID and TD properties is more significant at lower thickness ratio and the variation ceases out with the increase in thickness ratio. Further, it is also observed that the buckling strength of the panel is influenced by the nature of CNTs distribution. The panel with FG-X grading pattern is observed to have the highest buckling strength compared to the panels with other patterns of CNTs distribution (UD, FG-V, and FG-O). This is due to the fact that the stiffness of the panel with the FG-X pattern is high compared to other grading patterns as the concentration of CNTs are more at the extreme edges from the neutral axis of the panel. Similarly, the panel with the FG-O pattern is found to have lower buckling strength.

The curvature of the cylindrical panel plays an important role in deciding the buckling strength of the panel. Figure 4 shows the influence of the curvature ratio and in-plane temperature fields on the buckling strength of the panel. It is seen from Fig. 4 that the buckling strength is inversely proportional to the curvature ratio. As the curvature ratio increases, the moment of inertia of the panel decreases which decreases the bending resistance of the panel. Further, the influence of the in-plane temperature field is also seen on the panel with different curvature ratio. The panel exposed to Case(d) and Case(e) temperature fields generate low thermal stress thus observed to have a high buckling strength. As the expected influence of TD properties is more significant at lower curvature ratio which is due to high buckling temperature associated with lower curvature ratio. Irrespective of curvature ratio, the FG-X and FG-O grading pattern of CNTs results in higher and lower buckling strength respectively.

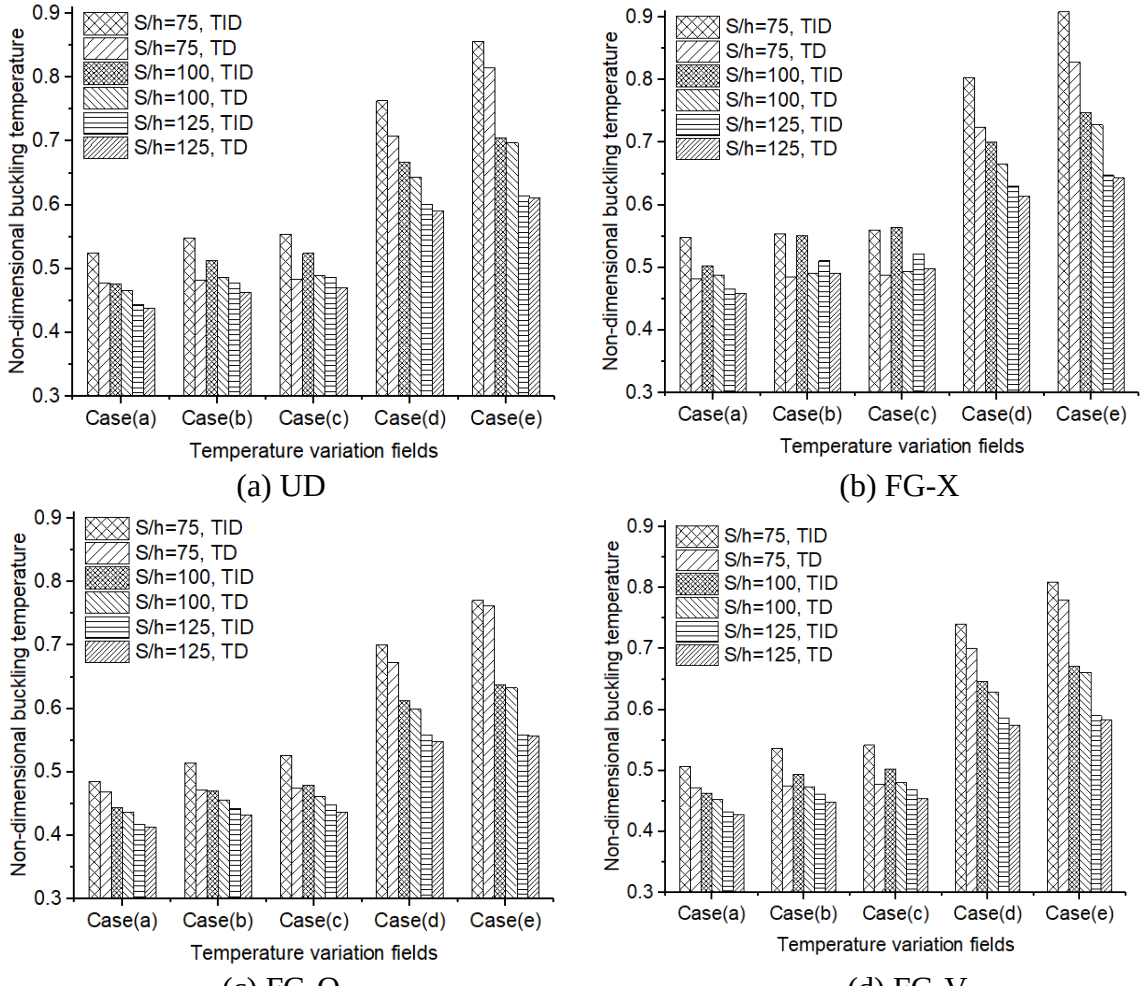

(a) UD (b) FG-X

(c) FG-O (d) FG-V

Fig. 3. Effect of temperature fields and thickness ratio on buckling strength of CCCC panel

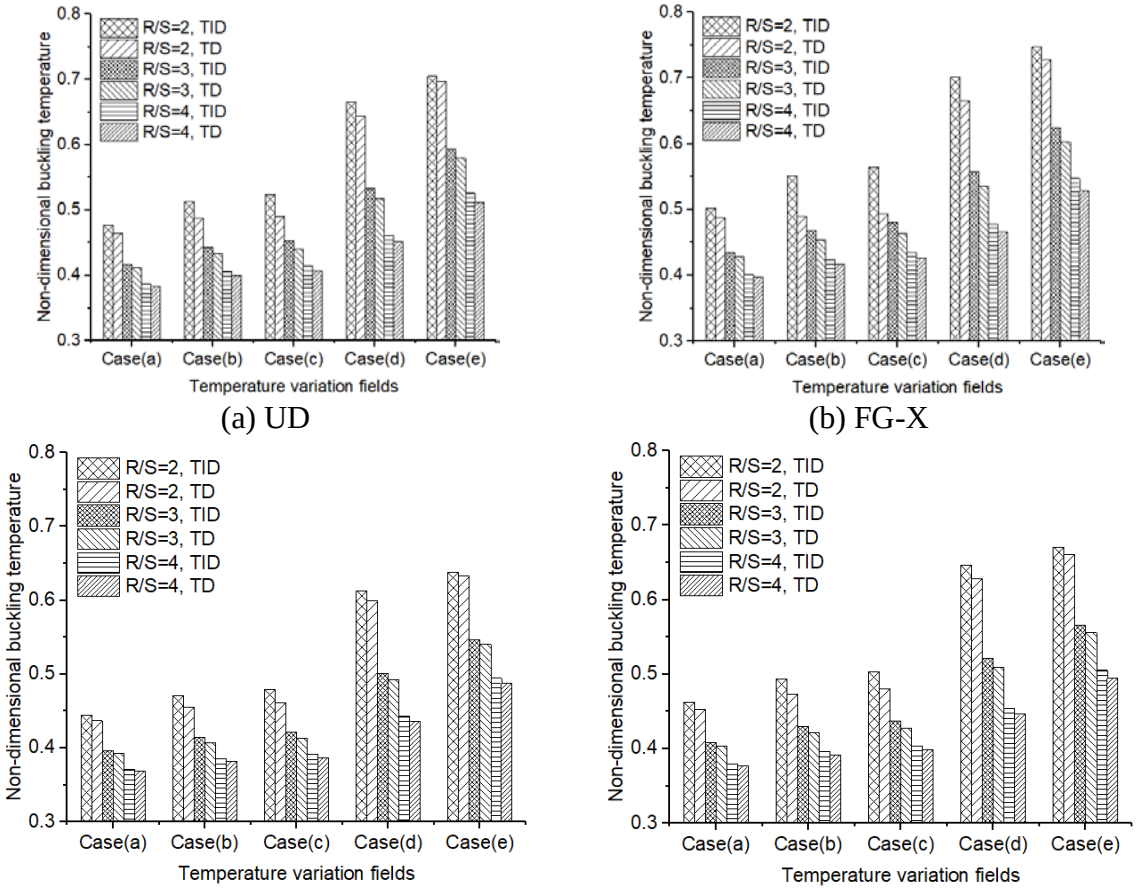

Fig. 4. Effect of temperature fields and curvature ratio on buckling strength of CCCC panel

Table 4 shows the combined effect of CNTs functional grading pattern, CNTs volume fraction, and TD properties, on the buckling strength of the panel with temperature fields. The buckling strength of the panel increases with the CNTs volume fraction irrespective of CNTs grading patterns and nature of temperature fields. This indicates that the structural stiffness of the panel enhances with the addition of CNTs. Panel with FG-X pattern and volume fraction of 0.28 is observed to have maximum buckling strength irrespective of the temperature fields analyzed. Irrespective of CNTs volume fraction, panel exposed to Case(a) and Case(d) temperature fields is observed with lowest and highest buckling strength respectively. Table 4 also shows the percentage difference of the buckling strength of the panel with TID and TD properties. It is noticed that a higher percentage difference is observed for the FG-X grading pattern at a higher volume fraction.

The influence of structural boundary constraints on the thermal buckling strength of the panel is presented in Table 5. As expected, CCCC panel is observed to have the lowest buckling strength compared to others. This is due to the fact that panel under CCCC boundary constraint does not allow any rotation and translation motion from any of its edges, thus free thermal expansion is completely restricted which leads to the development of high thermal stresses. However, the panel under CCFC boundary constraint allows free expansion from one of its edges and the amount of stress developed due to thermal load is partly released from the free edge making panel to buckle at a higher temperature. As observed in earlier cases, a panel with the FG-X grading pattern shows the highest buckling temperature irrespective of boundary constraints.

Table 4. Influence of CNTs volume fraction and temperature fields on the buckling temperature, T_{cr}^{*}

CNTs volume fraction	Temp field	CNTs grading pattern											
		UD			FG-X			FG-O			FG-V		
		TID	TD	%	TID	TD	%	TID	TD	%	TID	TD	%
0.12	Case(a)	0.477	0.465	2.34	0.502	0.488	2.89	0.444	0.437	1.71	0.462	0.453	2.11
	Case(b)	0.514	0.487	5.12	0.551	0.491	10.95	0.471	0.456	3.22	0.493	0.474	4.02
	Case(c)	0.524	0.490	6.53	0.564	0.493	12.59	0.479	0.462	3.62	0.503	0.480	4.51
	Case(d)	0.666	0.644	3.35	0.701	0.666	5.00	0.613	0.599	2.27	0.646	0.629	2.73
	Case(e)	0.705	0.697	1.11	0.747	0.728	2.53	0.638	0.633	0.84	0.671	0.661	1.43
0.17	Case(a)	0.483	0.472	2.26	0.511	0.500	2.28	0.450	0.443	1.57	0.470	0.460	2.02
	Case(b)	0.526	0.502	4.59	0.571	0.516	9.57	0.484	0.467	3.35	0.509	0.487	4.23
	Case(c)	0.538	0.510	5.24	0.587	0.519	11.48	0.493	0.475	3.77	0.520	0.495	4.74
	Case(d)	0.672	0.653	2.82	0.715	0.684	4.24	0.615	0.603	1.93	0.651	0.637	2.25
	Case(e)	0.707	0.705	0.33	0.757	0.747	1.37	0.635	0.632	0.50	0.670	0.662	1.17
0.28	Case(a)	0.513	0.483	5.79	0.560	0.487	12.93	0.480	0.470	2.21	0.506	0.490	3.16
	Case(b)	0.550	0.485	11.77	0.565	0.490	13.33	0.516	0.493	4.61	0.544	0.498	8.54
	Case(c)	0.561	0.488	13.01	0.571	0.493	13.70	0.526	0.499	5.16	0.556	0.501	9.95
	Case(d)	0.745	0.709	4.93	0.819	0.750	8.45	0.676	0.665	1.68	0.727	0.708	2.57
	Case(e)	0.796	0.784	1.58	0.885	0.836	5.55	0.698	0.702	-0.59	0.737	0.719	2.44

*Note: TID-Temperature independent; TD-Temperature dependent; Diff.: Difference

Table 5. Influence of boundary constraints on the buckling temperature, T_{cr}^{*}

Boundary constraints	Temp field	CNTs grading pattern											
		UD			FG-X			FG-O			FG-V		
		TID	TD	% Diff	TID	TD	% Diff	TID	TD	% Diff	TID	TD	% Diff
CCCC	Case(a)	0.477	0.465	2.34	0.502	0.488	2.89	0.444	0.437	1.71	0.462	0.453	2.11
	Case(b)	0.514	0.487	5.12	0.551	0.491	10.95	0.471	0.456	3.22	0.493	0.474	4.02
	Case(c)	0.524	0.490	6.53	0.564	0.493	12.59	0.479	0.462	3.62	0.503	0.480	4.51
	Case(d)	0.666	0.644	3.35	0.701	0.666	5.00	0.613	0.599	2.27	0.646	0.629	2.73
	Case(e)	0.705	0.697	1.11	0.747	0.728	2.53	0.638	0.633	0.84	0.671	0.661	1.43
CCFC	Case(a)	0.504	0.483	4.09	0.539	0.488	9.54	0.464	0.450	2.92	0.485	0.468	3.64
	Case(b)	0.524	0.487	6.96	0.565	0.491	13.13	0.478	0.460	3.75	0.502	0.478	4.71
	Case(c)	0.536	0.490	8.62	0.571	0.493	13.51	0.487	0.467	4.20	0.513	0.483	5.77
	Case(d)	0.853	0.757	11.22	0.890	0.759	14.72	0.802	0.746	6.97	0.841	0.765	9.04
	Case(e)	0.982	0.851	13.37	1.038	0.932	10.21	0.889	0.884	0.55	0.930	0.858	7.78

Note: TID-Temperature independent; TD-Temperature dependent; Diff.: Difference

The influence of different temperature fields on the buckling mode shape of a panel is investigated using MAC analysis. A CCCC cylindrical panel with UD grading pattern along with geometrical parameters *S/h*=100, *R/S*=2, and *L/S*=1 is considered for the MAC analysis. Figure 5 shows the MAC values for a panel exposed to different temperature field. It is found from the MAC values that the buckling mode of a panel is highly influenced by the in-plane temperature field. Buckling mode of a panel exposed to Case(a), Case(b), and Case(c) temperature fields are totally different from each other as indicated by lower MAC values. Further, it is also noticed from Fig. 5 that buckling mode of a panel exposed to Case(d) and Case(e) temperature field are very similar as indicated by higher MAC values. This can be attributed to the location of the heat source at the center of the panel under Case(d) and Case(e) temperature field.

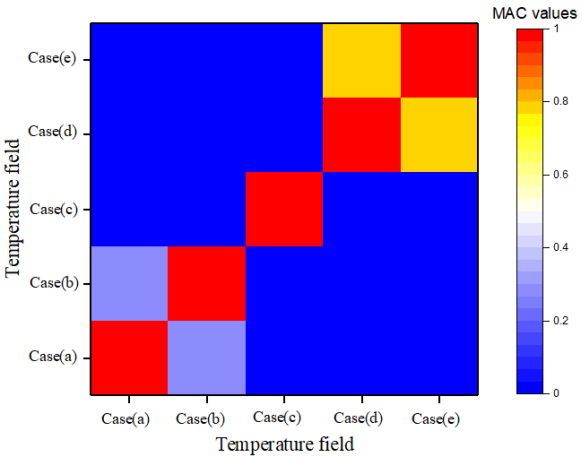

Fig. 5. Influence of temperature field on fundamental buckling mode

To investigate the influence of CNTs grading pattern on the buckling mode, a panel with CNTs volume fraction of 0.12 with geometrical parameters of *S/h*=100, *R/S*=2, and *L/S*=1. Figure 6 depicts the influence of CNTs grading pattern on the buckling mode of the panel exposed to Case(a) temperature field. It is clear from Fig. 6 that the buckling mode of the panel with UD, FG-O, and FG-V CNTs grading pattern is much similar whereas for FG-X grading it is distinct. This behavior is observed due to the high stiffness associated with the FG-X grading pattern. Further, the influence of CNTs volume fraction on the buckling mode is also analyzed. A panel with UD CNTs grading pattern is analyzed for the same. The MAC plot is shown in Fig. 7 to analyze the influence of CNTs volume fraction on buckling mode indicates that the buckling mode is not sensitive to CNT volume fraction.

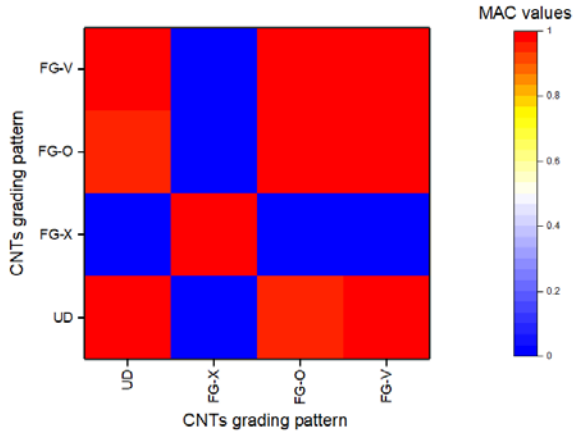

Fig. 6. Influence of CNTs grading pattern on fundamental buckling mode

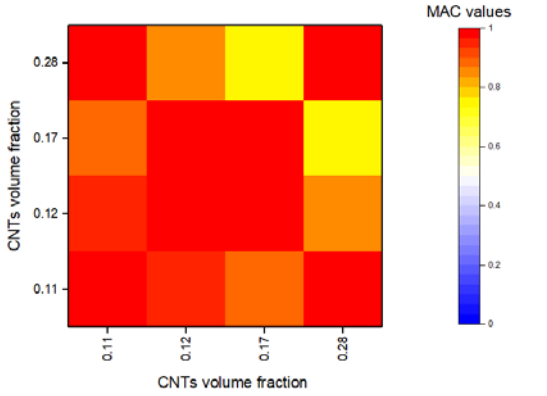

Fig. 7. Influence of CNTs volume fraction on fundamental buckling mode

Free vibration characteristics under thermal load. Figure 8 shows the influence of thermal load on the first fundamental frequency of the panel with TID and TD properties exposed to five different temperature fields. The thermal load is considered to be a function of critical buckling temperature (% T_{cr}) analyzed in the preceding section. Irrespective of CNTs grading pattern and temperature-dependent properties, fundamental frequency tends to decrease with the increase in temperature due to a reduction in structural stiffness of the panel. Reduction in frequencies is more significant at a temperature close to buckling temperature thus significant decrement is observed at 95% T_{cr}. It is also seen that the CNTs grading patterns enhances the fundamental frequencies of the panel wherein FG-X pattern is observed to have high fundamental frequencies compared to FG-O and FG-V grading pattern. Further, it is also found that the in-plane temperature field significantly influences the free vibration frequency.

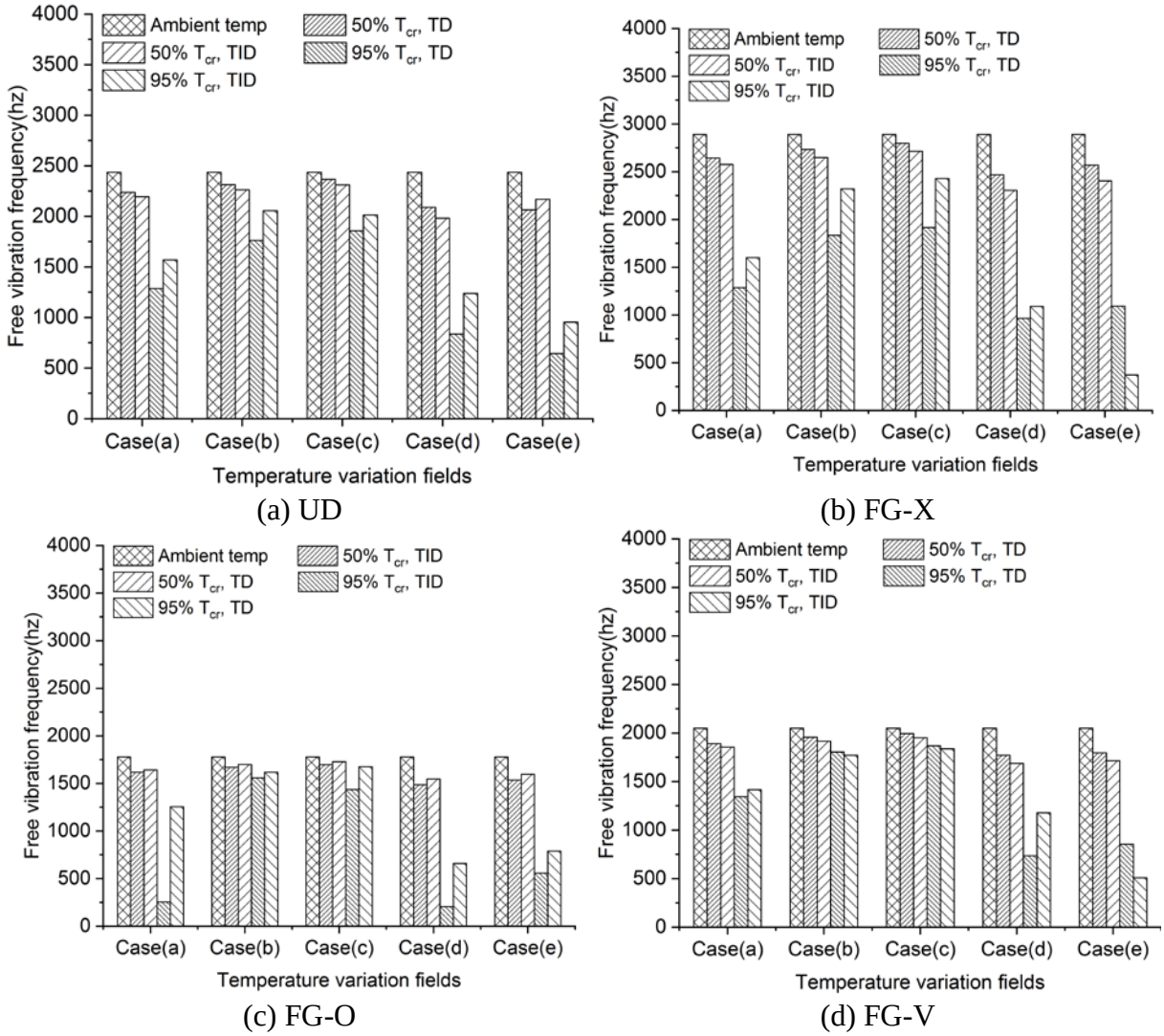

(a) UD (b) FG-X

(c) FG-O (d) FG-V

Fig. 8. Effect of thermal load (%T_{cr}) and temperature fields on first fundamental frequency

The influence of TD and TID properties on free vibration modes of the panel exposed to different temperature fields is shown in Table 6. It is observed that the free vibration mode shapes are significantly influenced by different temperature fields analyzed. Further, it is found that modes tend to shift along with the change in nodal and anti-nodal positions under different temperature fields. For example, mode 1 of CCCC panel having modal indices of (1,2) at ambient temperature changes to (3,2) at 95% of the critical buckling temperature under Case(a)

temperature field whereas the change in amplitude and nodal positions can be observed under Case(b) temperature field. Panel with TD properties is also analyzed for the change in mode shapes. As expected even with TD properties mode shapes and nodal position of free vibration modes changes with the temperature and its effect is more significant at 95% of critical buckling temperature.

Table 6. Influence of thermal load on the free vibration modes of the cylindrical panel with TD and TID properties

Temp. field	Modes	TID properties				TD properties			
		1	2	3	4	1	2	3	4
	Ambt temp	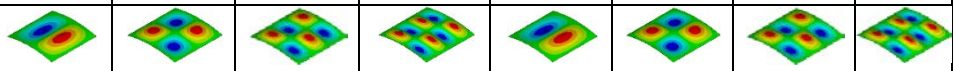							
Case(a)	$50\%T_{cr}$	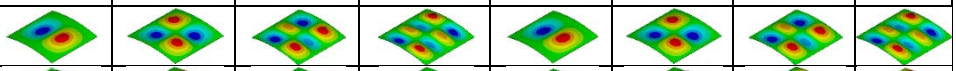							
	$95\%T_{cr}$	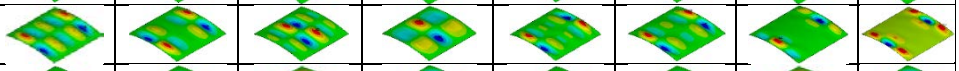							
Case(b)	$50\%T_{cr}$	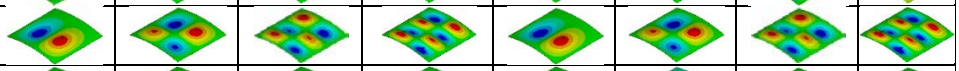							
	$95\%T_{cr}$	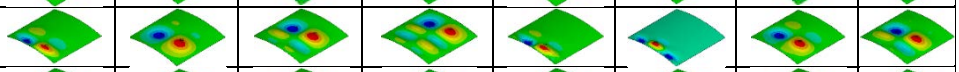							
Case(c)	$50\%T_{cr}$	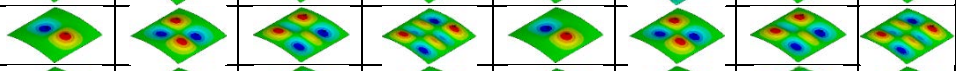							
	$95\%T_{cr}$	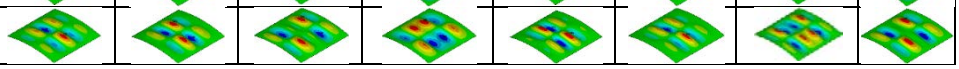							

Note: Red- max. displacement, Blue- min. displacement and others-inbetween

To analyze the variation of free vibration modes under the influence of temperature fields and temperature-dependent properties, MAC analysis is performed. Figures 9-10 depict the influence of thermal load, temperature-dependent properties, and in-plane temperature fields on the free vibration modes. It is clear from Table 6 and Fig. 9 that free vibration modes change with the in-plane temperature fields and found to be critical at a temperature close to the buckling temperature which is indicated by lower MAC values. Further, it is also found that the influence of temperature-dependent properties on the free vibration modes is significant at 95% of critical buckling temperature. The influence of thermal load on the first four free vibration modes is also studied in the present study using MAC analysis (Fig. 9). It is found that all four modes of a panel exposed to Case(b) temperature field have distinct mode shapes as indicated by lower MAC values. Further, it is also found that modes change with the thermal load and found to be significant at a temperature close to buckling temperature.

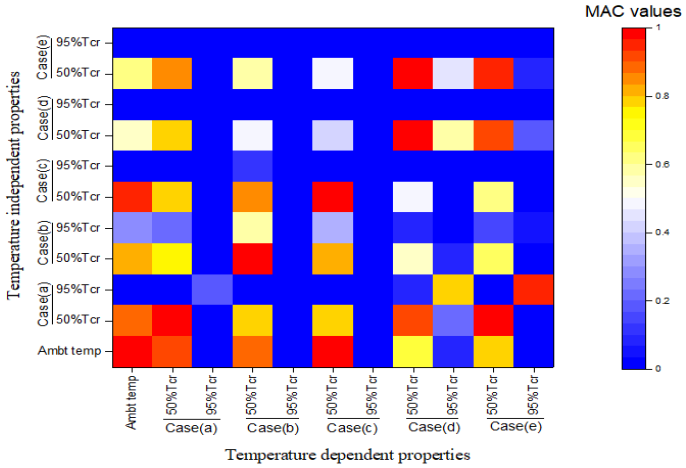

Fig. 9. Influence of temperature field on fundamental vibration mode

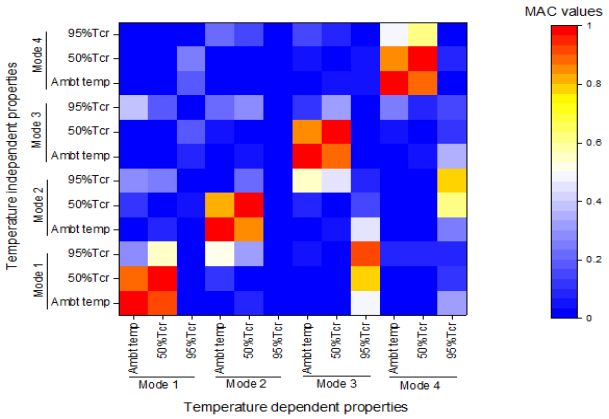

Fig. 10. Influence of thermal load on the first four free vibration modes

6. Conclusion

This paper deals with the investigation of buckling and free vibration behavior of functionally graded carbon nanotubes (FGCNT) reinforced composites cylindrical panels with TD properties exposed to different temperature fields using finite element method. Influence of geometrical parameters, in-plane temperature fields, CNTs grading pattern, CNTs volume fraction, and boundary constraints on the buckling and free vibration behavior of the panel are investigated in detail. It is found from the analysis that thermal buckling strength and free vibration frequencies of the panel are significantly influenced by the TD properties and variation of the temperature fields. It is also found that the effect of TD properties on the buckling strength is more significant on a panel at lower thickness and curvature ratio i.e. on the stiffer panel. CNTs grading pattern of type FG-X gives better buckling strength than the other pattern analyzed, irrespective of temperature fields. The effect of non-uniform temperature fields on the buckling temperature of the panel is more prominent on the stiffer panel. It is also noticed that free vibration frequencies of the panel analyzed decrease with the thermal load and variation is more significant at a thermal load close to buckling temperature. Shifting of nodal and anti-nodal lines and changing of modal indices with the rise in temperature has been observed through the present analysis. Further, jumping of free vibration modes is also noticed at a temperature close to the buckling temperature.

Acknowledgements. *No external funding was received for this study.*

References

[1] Zhao X, Liew KM. A mesh-free method for analysis of the thermal and mechanical buckling of functionally graded cylindrical shell panels. *Computational Mechanics*. 2010;45(4): 297-310.

[2] Talha M, Singh BN. Thermo-mechanical induced vibration characteristics of shear deformable functionally graded ceramic-metal plates using finite element method. *Proceedings of the Institution of Mechanical Engineers, Part C: Journal of Mechanical Engineering Science*. 2011;225(1): 50-65.

[3] Shen HS. Thermal buckling and postbuckling behavior of functionally graded carbon nanotube-reinforced composite cylindrical shells. *Composites Part B: Engineering*. 2012;43(3): 1030-1038.

[4] Attia A, Tounsi A, Bedia EA, Mahmoud SR. Free vibration analysis of functionally graded plates with temperature-dependent properties using various four variable refined plate theories. *Steel and composite structures*. 2015;18(1): 187-212.

[5] Ahmadi SA, Pourshahsavari H. Three-dimensional thermal buckling analysis of functionally graded cylindrical panels using differential quadrature method (DQM). *Journal of Theoretical and Applied Mechanics*. 2016;54(1): 135-147.

[6] Bouderba B, Houari MS, Tounsi A, Mahmoud SR. Thermal stability of functionally graded sandwich plates using a simple shear deformation theory. *Structural Engineering and Mechanics*. 2016;58(3): 397-422.
[7] Zhang LW, Lei ZX, Liew KM, Yu JL. Static and dynamic of carbon nanotube reinforced functionally graded cylindrical panels. *Composite Structures*. 2014;111: 205-212.
[8] Lei ZX, Zhang LW, Liew KM, Yu JL. Dynamic stability analysis of carbon nanotube-reinforced functionally graded cylindrical panels using the element-free kp-Ritz method. *Composite Structures*. 2014;113: 328-338.
[9] Mirzaei M, Kiani Y. Free vibration of functionally graded carbon nanotube reinforced composite cylindrical panels. *Composite Structures*. 2016;142: 45-56.
[10] Wang P, Huang X, Wang Z, Geng X, Wang Y. Buckling and post-buckling behaviors of a variable stiffness composite laminated wing box structure. *Applied Composite Materials*. 2018;25(2): 449-467.
[11] Dikshit MK, Engle PE. Investigation Of Mechanical Properties Of Cnt Reinforced Epoxy Nanocomposite: A Molecular Dynamic Simulations. *Materials Physics and Mechanics*. 2018;37(1): 7-15.
[12] Shen HS, Xiang Y. Nonlinear vibration of nanotube-reinforced composite cylindrical shells in thermal environments. *Computer Methods in Applied Mechanics and Engineering*. 2012;213: 196-205.
[13] Jeyaraj P. Buckling and free vibration behavior of an isotropic plate under nonuniform thermal load. *International Journal of structural stability and dynamics*. 2013;13(3): 1250071.
[14] George N, Jeyaraj P, Murigendrappa SM. Buckling and free vibration of nonuniformly heated functionally graded carbon nanotube reinforced polymer composite plate. *International Journal of Structural Stability and Dynamics*. 2017;17(6): 1750064.
[15] George N, Jeyaraj P, Murigendrappa SM. Buckling of non-uniformly heated isotropic beam: Experimental and theoretical investigations. *Thin-Walled Structures*. 2016;108: 245-255.
[16] George N, Jeyaraj P. Nonuniform Heat Effects on Buckling of Laminated Composite Beam: Experimental Investigations. *International Journal of Structural Stability and Dynamics*. 2018;18(12): 1850153.
[17] Bhagat VS, Pitchaimani J, Murigendrappa SM. Buckling and dynamic characteristics of a laminated cylindrical panel under non-uniform thermal load. *Steel and Composite Structures*. 2016;22(6): 1359-1389.
[18] Bhagata VS, Pitchaimani J, Murigendrappa SM. Buckling and vibration behavior of a non-uniformly heated isotropic cylindrical panel. *Structural Engineering and Mechanics*. 2016;57(3): 543-567.
[19] Bhagat V, Jeyaraj P. Experimental investigation on buckling strength of cylindrical panel: Effect of non-uniform temperature field. *International Journal of Non-Linear Mechanics*. 2018;99: 247-257.
[20] Li X, Gao H, Scrivens WA, Fei D, Xu X, Sutton MA, Reynolds AP, Myrick ML. Reinforcing mechanisms of single-walled carbon nanotube-reinforced polymer composites. *Journal of Nanoscience and Nanotechnology*. 2007;7(7): 2309-2317.
[21] Seidel GD, Lagoudas DC. Micromechanical analysis of the effective elastic properties of carbon nanotube reinforced composites. *Mechanics of Materials*. 2006;38(8-10): 884-907.
[22] Esawi AM, Farag MM. Carbon nanotube reinforced composites: potential and current challenges. *Materials & design*. 2007;28(9): 2394-2401.
[23] Fidelus JD, Wiesel E, Gojny FH, Schulte K, Wagner HD. Thermo-mechanical properties of randomly oriented carbon/epoxy nanocomposites. *Composites Part A: Applied Science and Manufacturing*. 2005;36(11): 1555-1561.

[24] Librescu L, Oh SY, Song O. Thin-walled beams made of functionally graded materials and operating in a high temperature environment: vibration and stability. *Journal of Thermal Stresses*. 2005;28(6-7): 649-712.
[25] Aragh BS, Barati AN, Hedayati H. Eshelby–Mori–Tanaka approach for vibrational behavior of continuously graded carbon nanotube-reinforced cylindrical panels. *Composites Part B: Engineering*. 2012;43(4): 1943-1954.
[26] Shen HS. Nonlinear bending of functionally graded carbon nanotube-reinforced composite plates in thermal environments. *Composite Structures*. 2009;91(1): 9-19.
[27] Han Y, Elliott J. Molecular dynamics simulations of the elastic properties of polymer/carbon nanotube composites. *Computational Materials Science*. 2007;39(2): 315-323.
[28] Zhu P, Lei ZX, Liew KM. Static and free vibration analyses of carbon nanotube-reinforced composite plates using finite element method with first order shear deformation plate theory. *Composite Structures*. 2012;94(4): 1450-60.
[29] Jeng-Shian C, Wei-Chong C. Thermal buckling analysis of antisymmetric laminated cylindrical shell panels. *International Journal of Solids and Structures*. 1991;27(10): 1295-309.
[30] Malekzadeh P, Vosoughi AR, Sadeghpour M, Vosoughi HR. Thermal buckling optimization of temperature-dependent laminated composite skew plates. *Journal of Aerospace Engineering*. 2014;27(1): 64-75.
[31] Pastor M, Binda M, Harčarik T. Modal assurance criterion. *Procedia Engineering*. 2012;48: 543-548.
[32] Boroujerdy MS, Naj R, Kiani Y. Buckling of heated temperature dependent FGM cylindrical shell surrounded by elastic medium. *Journal of Theoretical and Applied Mechanics*. 2014;52(4): 869-881.
[33] Mirzaei M, Kiani Y. Thermal buckling of temperature dependent FG-CNT reinforced composite conical shells. *Aerospace Science and Technology*. 2015;47: 42-53.